JOURNAL OF APPLIED ELECTROCHEMISTRY **27** (1997) 1079–1087

Analysis of charge rejection by an ionomeric plasma polymerized film for biomedical sensor applications

R. C. TUCKER[*], I. SONG[‡], J. H. PAYER[‡], R. E. MARCHANT[*§]

[*] *Department of Biomedical Engineering and* [‡] *Department of Materials Science & Engineering, Case Western Reserve University, Cleveland, OH 44106, USA*

Received 6 March 1996; revised 7 September 1996

A thin novel ionomeric plasma polymerized perfluoroallylphosphonic acid (PPPAPA) film has been developed to improve biomedical sensor ionic selectivity. PPPAPA films (average thickness 470 nm) were deposited on gold wire electrodes. The ability of PPPAPA to reject a negative organic interferant, ascorbate, was compared with the transport of a positive organic ion, dopamine, using cyclic voltammetry (CV) and chronocoulometry. From analysis of CV data, PPPAPA film-coated gold electrodes showed a 50% reduction in current density response for ascorbate and a 5% reduction in response for dopamine compared with bare gold electrodes. Apparent analyte diffusion coefficients, calculated from chronocoulometry of PPPAPA film-coated electrodes, showed a 50% reduction for ascorbate transport compared with dopamine. The results demonstrate that PPPAPA films are ion-selective and may have potential application as a biomedical sensor coating.

1. Introduction

Amperometric biomedical sensors are designed to provide instantaneous information of a wide variety of physiologically important analytes. For example, oxygen sensors can diagnose hypoxia during surgery, and glucose sensors can provide feedback for diabetics [1]. In simple amperometric sensors, the analyte undergoes a redox reaction to induce current at the working electrode proportional to the analyte concentration, as described by Faraday's law. Unfortunately, conventional biomedical sensors show poor long-term stability and reproducibility when implanted. This may be due to organic fouling, noise from interferant ions, or deactivation of the sensor's transducing mechanisms through processes such as enzyme degradation.

An interferant ion encountered when measuring the catecholamine neurotransmitter dopamine *in vivo* is ascorbate. Dopamine is released from neurons of the central nervous system, in the concentration range of 50 nM [2, 3], and can be detected electrochemically by the exchange of two electrons when dopamine oxidizes to dopamine *o*-quinone [4, 5]. Ascorbic acid, which is ionized to ascorbate at physiological pH, is a strong electrochemical interferant: it occurs in large concentrations (~200 μM) in the brain and is highly oxidizable at low potentials (around +350 mV vs SCE). Electrochemical oxidation of ascorbate releases two electrons, and then undergoes rapid, irreversible hydrolysis to form dehydroascorbic acid [6, 7]. Ascorbate is also a common interferant in peroxidase-enzyme based sensors by competing in a homogeneous reaction with hydrogen peroxide [8].

To detect an analyte in the presence of interfering ions, the working electrode surface can be modified to block the interferant without affecting the transport of the analyte to the electrodes surface, thereby improving the sensor stability and selectivity [9]. This may be done by converting surface groups electrochemically [10, 11], applying self-assembled monolayers [12, 13], or depositing polymeric films [14–17]. A common polymeric film used to surface-modify electrodes is Nafion® (DuPont), a perfluoroalkylsulfonated resin, and can be deposited by dip- or spin-coating. Nafion® has been used to provide improved ion selectivity by rejecting anions with its negatively charged sulfonic acid groups [18–20]. This property has been utilized to improve *in vivo* detection of many different analytes in the presence of ascorbate [21–23].

Unfortunately, Nafion® has a few limitations for use as a general biomedical sensor coating. The dip-coating method for depositing the Nafion® on electrodes surfaces is prone to much thickness variability [24] and has difficulty ensuring uniformity on cylindrical electrodes [25, 26]. Nafion® must be cured at high temperatures (~120 °C) for stability, but this leads to decreased permeability and diffusion coefficients [27] and still shows poor adhesion [18, 24]. Upon implantation, Nafion®-coated electrodes show decreased sensitivity, reducing its maximum current response to 50–60% of its original magnitude [23, 24]. This sensitivity loss is seen when testing in whole blood [28] and is probably due to protein adsorption.

An alternative approach, described in this report, is to employ novel plasma polymerized perfluorinated ionomeric films, which can be deposited uniformly

§ To whom correspondence should be addressed.

directly on many different electrode surfaces [29–32]. This batch process allows multiple electrodes to be coated with well-controlled deposition rates without the need for post-deposition curing. These films form an intimate polymer-substrate interface with good adhesion and high crosslink densities, which should facilitate stability and size selectivity [33]. We have reported previously [34] on a novel ionomeric plasma polymerized perfluoroallyphosphonic acid (PPPAPA) film. This film shows good adhesion to gold surfaces and can be made very thin (< 100 nm) for fast transient response. The film is extremely hydrophilic [35], which may limit fouling from plasma protein adsorption [36, 37].

In this work, we examine the electrochemical and ion transport properties of the PPPAPA ionomer. PPPAPA films were characterized by ellipsometry, Fourier transform infrared spectroscopy (FTIR), X-ray photoelectron spectroscopy (XPS), and atomic force microscopy (AFM). The electrochemical response of gold electrodes with and without the PPPAPA film were tested with the positively charged neurotransmitter, dopamine, and the negatively charged interferant, ascorbate. Since these two compounds have similar molecular weight, size, and diffusion coefficient in water (Table 1), different amperometric or coulometric responses provide a quantitative indicator of charge selectivity. Negative ion rejection and positive ion transport by the PPPAPA film were measured using cyclic voltammetry. Chronocoulometry was used to estimate the apparent diffusion coefficient of each ion and quantify transport through the PPPAPA film.

2. Experimental details

2.1. *Materials*

Perfluoroallylphosphonic acid (PAPA) ($F_2C{=}CFCF_2P(O)(OH)_2$) monomer was provided by D. Burton (Department of Chemistry, University of Iowa) and stored under argon at –5 °C. Dopamine (3-hydroxytyramine hydrochloride) and ascorbic acid (reagent grade, Sigma) were used as-received. Ultrapure water used was obtained from a Milli-RO 10 plus (Millipore) purification system followed by ultra purification with a Milli-Q UV plus (Millipore) water system. This provides water with a resistivity of greater than 18 MΩ cm, with total organic carbon levels lower than 5 parts per 10^9. Reagent grade sulfuric acid, acetone, methanol, and ethanol were used as-received. A stock solution of NBS phosphate buffer (pH 7.4, ionic strength 0.13 M) was prepared by mixing reagent grade disodium phosphate and monopotassium phosphate (Fisher Scientific) [38]. The absence of chloride ions in the NBS phosphate buffer simplified the electrochemical experiments by eliminating competitive adsorption complications [39].

Plasma reactor glassware was cleaned overnight in a sulfuric acid/Nochromix powder (Godax Laboratories) solution, washed in diluted Liquinox soap solution (Alconox), rinsed with tap water, Millipore water, and ethanol, and dried at 100 °C. All stainless steel vacuum line fittings were soaked in ethanol overnight and dried at 100 °C.

2.2. *Substrates*

Substrates used as support for depositing PPPAPA films included glass microslides, gold-coated silicon wafers, germanium internal reflection elements, and gold wire electrodes. Glass microslides (25 mm × 75 mm) were cleaned by immersion in concentrated sulfuric acid overnight, followed by rinsing with distilled water and methanol. This procedure provided reproducibly clean hydrophilic glass substrates. Gold-coated silicon wafers were prepared at the Electronics Design Center at Case Western Reserve University. Silicon wafers (1 1 1 face, 2 inch diameter, Wacker, Inc.) were cleaned using an 80 °C solution of deionized water:hydrogen peroxide:ammonium hydroxide (5:2:1 mixture) for 5 min, spin rinsed in 18 MΩ deionized water for 2 min, dried under nitrogen, ultrasonicated for 5 min in trichloroethylene, acetone, and methanol, spin rinsed in 18 MΩ deionized water for 2 min, and dried under nitrogen. Silicon wafers were gold-coated by heating the wafers to 100 °C and depositing a 5 nm chromium adhesion layer on the clean silicon wafer using a thermal evaporation system (model 409, Consolidated Vacuum Corp.), followed by evaporation deposition of ~200 nm of gold. Wafers were then scored into 1 cm × 2 cm rectangles using a diamond saw (model 1100, Microautomation). A length of gold wire (0.5 mm diameter, 99.999 % pure, Aldrich Chem.) was used as the working electrode for all electrochemical experimentation. Each electrode was cleaned by flame annealing, followed by quenching in water.

2.3. *Plasma polymerization system and procedure*

Plasma polymer films were prepared using a radio-frequency (RF) plasma system described previously

Table 1. Physical characteristics of dopamine and ascorbic acid

Analyte	*Charge*	*Molecular Weight*	*Max. cross sectional area* /Å^{2*}	10^5 *D* (H_2O) /cm^2 s^{-1} [57]	$10^9 D_{app}$ (*Nafion*®) /cm^2 s^{-1} [52]
Dopamine	+	189.64	45.4	0.60	2.3
Ascorbate	–	176.12	44.7	0.53	<0.1

* Calculated using a molecular modelling package (Biosym) on a Silicon Graphic Instrument computer

[40]. The reaction chamber was capacitively coupled using two 12.5 mm copper strips spaced 13 cm apart and connected to a RF power supply (model HFS251S, RF Plasma Products). This coupling system provided a uniform, intense glow throughout the reactor under the conditions used in this study.

All samples were mounted on clean microslides affixed to a glass rod tray. The tray was placed in the reactor so that the leftmost samples are 1 mm away from the leftmost copper strip. PAPA monomer (~5 ml) was placed in a round bottomed flask (100 ml) and heated to approximately 90 °C with a heating mantle. The flask was connected to an inlet line with a glass stopcock fitted with a Teflon plunger and Viton o-rings (Ace Glass). The glass inlet line extends 14.5 cm into the reaction chamber, to allow a uniform flow pattern.

The glass reactor chamber (3300 cm^3) was evacuated overnight to remove residual adsorbed gases, stabilized at a base pressure around 7 mtorr, and examined for leaks. The monomer was degassed under vacuum for 4 or 5 freeze-thaw cycles by liquid nitrogen and a heating mantle. The substrate surfaces were pretreated with an argon glow discharge carried out for 5 min at 40 W net discharge power, 30 mtorr pressure, and argon flow rate approximately 1.9 cm^3 min^{-1} at standard temperature and pressure (STP). After the argon treatment, the reactor was evacuated, and the monomer was introduced at a constant preplasma flow rate of 0.073 cm^3 (STP) min^{-1}, calculated from the measured pressure rise in the reaction chamber with the shutoff valve closed [41]. Plasma polymerization reactions were carried out at a constant pressure (30 mtorr) and net discharge power (40 W) until thick film deposition was observed from film interference patterns on silicon wafers after 60 min. The plasma was extinguished, and the reactor pressure was maintained at 30 mtorr for 5 min. The monomer flow was then stopped, and the reactor was allowed to remain at the base pressure overnight. The reactor was filled to atmospheric pressure with argon, and the treated samples were removed from the reactor and stored in a desiccator.

2.4. *Surface characterization methods*

Film thicknesses of the plasma polymerized films deposited on the gold-coated silicon wafers were determined by ellipsometry. Measurements were made with an ellipsometer (model L117, Gaertner) with a helium/neon source (three measurements per sample), and the thickness was determined from the data using a FORTRAN program [42]. For this calculation, the index of refraction of the plasma polymer was assumed to be 1.54, which is the mean value determined for similar plasma polymer films prepared with this reaction system [43, 44].

To characterize the elemental composition of PPPAPA film deposited on the gold-coated silicon wafers, X-ray photoelectron spectroscopy (XPS) was performed using a Physical Electronics PHI 5600 X-ray photoelectron spectrometer. The incident radiation consisted of monochomatized aluminium K_α X-rays (1486.8 eV) with a take-off angle of 45 °. A specimen neutralizer (model 04-090, Physical Electronics) was used to keep samples from charging. Approximately 4 V was applied between the neutralizer and the sample, which was adjusted until the C1s peak centred at 285.0 eV. For survey scans, the binding energy range was swept from 1100 to 0 eV at 20 ms/step and 0.4 eV/step.

Fourier transform infrared (FTIR) spectra of PPPAPA films were obtained using an infrared spectrometer (model FTS-40, Digilab) equipped with an attenuated total internal reflection (ATR) optical accessory (model 50, Wilkes Scientific) and a mercury–cadmium–telluride (MCT) detector. The plasma polymer films were deposited onto 50 mm × 20 mm × 2 mm, 45° trapezoidal germanium internal reflection elements that were cleaned by polishing with alumina paste (Buehler gamma micropolish II, 0.05 μm particle size) on a velour pad and rising with Millipore water and methanol. Spectra were obtained with a resolution of 8 cm^{-1} by sample averaging 1024 scans.

Atomic force microscopy (AFM) topographical imaging was performed under ambient conditions using a Bioscope AFM (Digital Instruments) operating in tapping mode. The gold-coated silicon wafer samples were first attached to 15 mm metal discs using cyanoacrylate adhesive, and the metal disks were mounted on glass microscope slides using double-sided adhesive. Images were obtained with 125 μm long, single beam silicon cantilevers (Digital Instruments). After engagement on the sample, the setpoint value, scan rate, scan speed and feedback control values were adjusted to minimize tip attenuation to prevent sample damage as well as to eliminate hysteresis between the forward and return traces of the probe. Images were subjected to a 3 × 3 low pass filter, a zero order flatten, and a second order planefit. Root mean square (RMS) roughness values and maximum Z-range values were analysed with Digital Instrument system software.

2.5. *Electrochemical methods*

Cyclic voltammetry was performed in a conventional three compartment glass cell under ambient conditions with nitrogen purging. Prior to experimentation, the cell was cleaned by soaking in boiling acid (1:1 nitric acid:sulfuric acid) and left to cool overnight, rinsed by soaking in boiling distilled water and allowed to cool overnight, and steam-cleaned for about 5 min before use. After each experiment, the cell was rinsed in distilled water, steam-cleaned for about 5 min, rinsed in distilled water, and filled with fresh phosphate buffer. A separate glass cell was used for each analyte. A gold wire counter electrode was separated from the working electrode chamber by a glass frit. A saturated calomel reference electrode (SCE) was connected to the working electrode

Table 2. Elemental composition of PPPAPA films

PPPAPA polymer films						
Sample	*C1s*	*N1s*	*O1s*	*P2p*	*F1s*	*Au4f*
PPPAPA*	37.0 ± 2.2	9.6 ± 5.1	19.7 ± 1.4	4.6 ± 0.8	29.1 ± 4.4	0.0 ± 0.0
PAPA†	25.0	0.0	25.0	8.3	41.7	0.0

* Values are means ± standard deviations
† Theoretical value for PAPA monomer
PPPAPA: plasma polymerized perfluoroallylphosphonic acid
PAPA: perfluoroallylphosphonic acid

chamber with a cracked stopcock bridge filled with NBS phosphate buffer to prevent contamination of the electrolyte with chloride from the reference electrode. A Luggin capillary was used with the tip approximately 3 cm below the centre of the working electrode. Fresh analyte was made before each experiment.

Validation of the electrochemical system was performed by taking voltammograms of bare gold wire as a working electrode. Each sample was immersed in solution to a depth 5 to 10 mm with a *z*-positioner, allowing an approximate geometrical area to be calculated. A cyclic voltammogram (CV) of the wire was taken at room temperature in nitrogen-purged NBS phosphate buffer with a voltammograph (Model CV-27, BAS) and recorded on a *X–Y* recorder (Model WX 1000, Watanabe). The CV was measured between –200 mV and +600 mV vs SCE at a scan rate of 100 mV s^{-1}. The first cycle and every other cycle were recorded until stable. This procedure was repeated as aliquots of dopamine or ascorbic acid were added. In a similar manner, experiments were performed with PPPAPA coated gold wire electrodes. The films were soaked in NBS phosphate buffer for a minimum of 3 min before addition of the dopamine or ascorbic acid aliquots.

To calculate apparent diffusion coefficients of each analyte through the film, chronocoulometry experiments were made. A potential step between –50 and +350 mV vs SCE was applied to the bare and film-coated gold working electrode by the BAS voltammograph. The resulting current and charge were plotted on a strip chart recorder (model 3056, YEW). For analysis, raw coulometry data was measured from strip chart recordings in intervals of 0.5 seconds up to 2.5 s to approximate semi-infinite linear diffusion conditions [45].

3. Results

3.1. *Surface characterization*

An effective charge selective film must have complete film coverage and functional (unhindered) ionomeric groups. Therefore, multiple techniques including ellipsometry, XPS, FTIR, and AFM, were used to characterize the films and verify complete coverage before electrochemical experimentation. The thickness of the PPPAPA films calculated from ellipsometry data of the gold-coated silicon wafers was 470 ± 90 nm, yielding an estimated mean deposition rate 8.0 ± 1.5 nm min^{-1}.

The atomic composition of the PPPAPA films, determined by XPS, are shown in Table 2. PPPAPA contains carbon, fluorine, oxygen, and phosphorus, consistent with the PAPA monomer and previous PPPAPA films [34, 35]. Some nitrogen is present in the film, probably derived from incomplete monomer degassing, but the amount is consistent with our previous studies [34, 35]. The absence of underlying gold signal (Au4f at 83 eV) suggests a film thickness greater than the escape depth for photoelectrons with kinetic energy of ~1400 eV. This thickness is at least 2 nm [46].

The FTIR spectra for the PAPA monomer and PPPAPA are shown in Fig. 1 and are consistent with previous detailed characterization studies of these films [34, 35, 47]. This spectrum indicates retention of ionomeric groups from PAPA, exemplified by the strong broad peak between 1800 and 1500 cm^{-1} attributed to ν(O–H) in $P(O)(OH)_2$ and the band at 1040 cm^{-1} attributed to ν(P–O) in P-OH. A strong broad band between 1300 and 1100 cm^{-1} is attributed

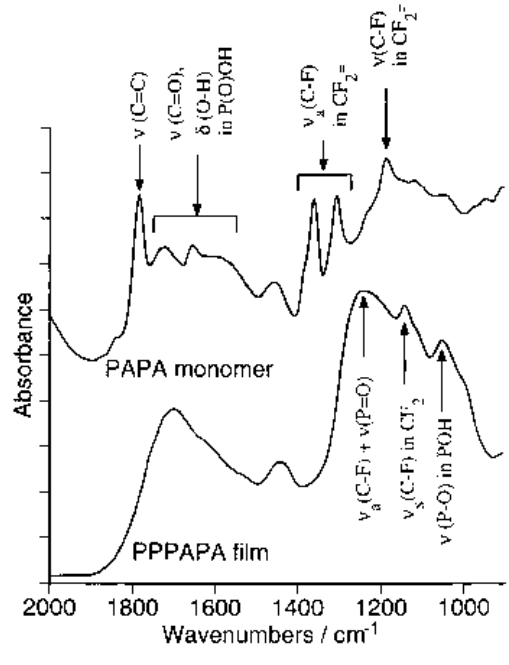

Fig. 1. FTIR, 2000–900 cm^{-1} region of PAPA monomer and plasma polymerized PAPA film (PPPAPA).

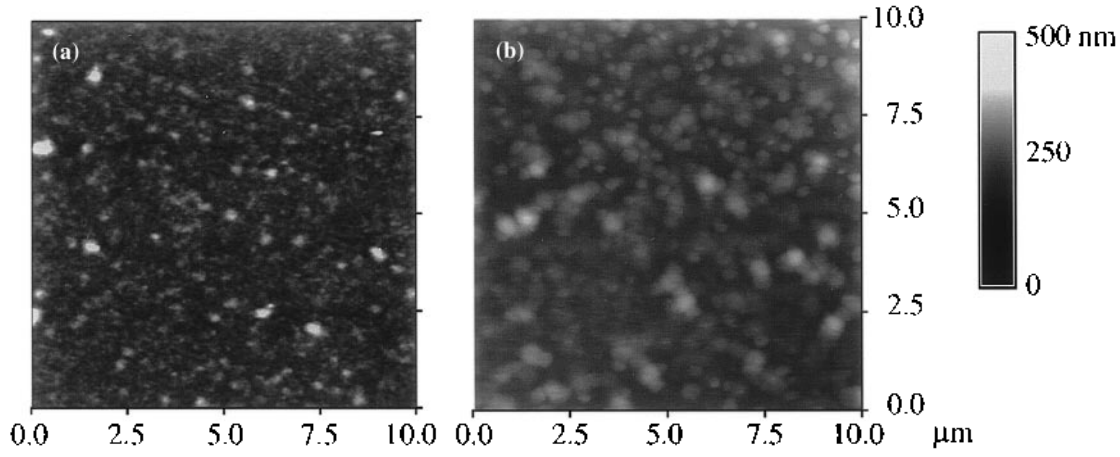

Fig. 2. AFM tapping mode images taken under ambient condition (10 μm lateral scan size and 500 nm height range). (a) Evaporation-deposited gold (~200 nm) on a silicon wafer. Calculated z-range and RMS roughness are 80 and 6 nm, respectively. (b) PPPAPA deposited film on evaporation-deposited gold on a silicon wafer. Calculated z-range and RMS roughness are 110 and 14 nm, respectively.

to C–F stretching from the fluorocarbon backbone. All adsorption peaks indicative of C=C in the monomer at 1786,1350, and 1300 cm^{-1} are not present in PPPAPA, as expected for successful polymerization.

AFM tapping mode was used to determine film topography and to estimate film coverage. The topography of evaporation-deposited gold on a silicon wafer can be compared before (Fig. 2(a)) and after (Fig. 2(b)) application of the PPPAPA film. The bare gold substrate shows a relatively smooth surface, with a z-range and RMS roughness calculated to be 80 and 6 nm, respectively. The PPPAPA film deposited on the gold-coated silicon wafer has a rougher surface than the original substrate, with a z-range and RMS roughness value 110 and 14 nm. Because the z-range is less than the film thickness calculated by ellipsometry (~470 nm), complete film coverage with good uniformity is indicated.

The surface characterizations provide evidence that a complete and uniform ionomeric film was deposited. While ionomeric groups are indicated from analysis of infrared spectra, further electrochemical experiments are necessary to establish that the ionomeric groups are functional for negative ion rejection.

3.2. *Cyclic voltammetry*

Cyclic voltammetry was used to measure the flux of dopamine and ascorbate through PPPAPA, indicated by an increase in current at their peak oxidation potentials. After the film was deposited on the gold wire electrodes, a voltammogram of each electrode was measured in NBS phosphate buffer in the presence and absence of dopamine (Fig. 3). A typical voltammogram shows that PPPAPA incites no CV response, but addition of dopamine does show an electrochemical response, proving dopamine can pass through the film. A comparison of the bare gold electrode's CV with and without the PPPAPA film indicates that the current density response is unaffected by the film, and the dopamine flux to the electrode surface is minimally affected by the PPPAPA film; on average a 5% decrease in current density is observed by applying the film. In voltammograms of ascorbate at a bare gold electrode (Fig. 4), no reduction peak is evident, because ascorbate oxidizes irreversibly. The peak ascorbate oxidation current measured on the PPPAPA-modified gold electrodes is much less than that on the bare gold. Ascorbate oxidation peaks are noticeable on the PPPAPA modified gold electrodes, but the magnitude of actual oxidation current is considered small when the double layer charging current is discounted, as seen on PPPAPA modified gold electrodes in absence of ascorbate (dotted curve). This indicates qualitatively that the transport of ascorbate to the electrode surface is hindered significantly by the PPPAPA film.

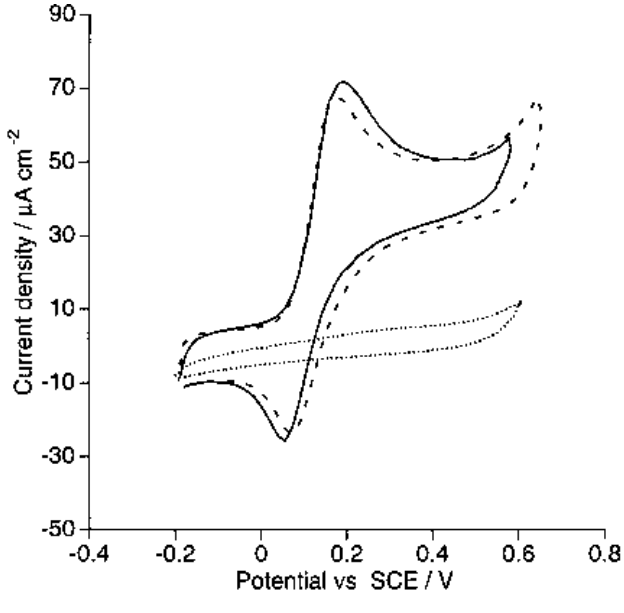

Fig. 3. Cyclic voltammograms (CV) of gold in anaerobic aqueous phosphate buffer (pH 7.4) of (·····) a PPPAPA film coated gold electrode without analyte; (- - - -) a bare gold electrode with 100 μM dopamine (DA); and (——) a PPPAPA film coated gold electrode with 100 μM dopamine.

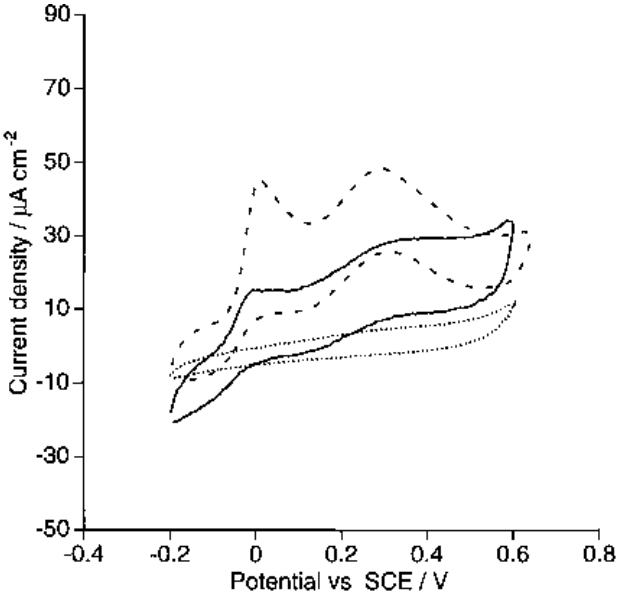

Fig. 4. Cyclic voltammograms (CV) of gold in anaerobic aqueous phosphate buffer (pH 7.4) of (·····) a PPPAPA film coated gold electrode without analyte; (- - - -) a bare gold electrode with 100 μM ascorbate (AA); and (——) a PPPAPA film coated gold electrode with 100 μM ascorbate (AA).

To determine each electrode's response for a variety of concentrations, the current density as a function of dopamine with and without the plasma film was measured as shown in Fig. 5(a). Each data point was obtained by taking the diffusion limited current density at + 350 mV vs SCE as a function of dopamine concentration. Each point on the graph is an average of three different experiments, and the error bars are the standard deviations. The resulting slope, drawn using the method of least squares, provides an indication of the sensor's sensitivity. This figure indicates that the sensitivity of gold electrodes was decreased by only 5% upon the application of the ionomeric plasma film. A similar sensitivity curve was obtained for the ascorbate solution as shown in Fig. 5(b). In this case, the sensitivity (determined by the slope) was decreased by an average of 50%, by applying the ionomeric plasma film. This result indicates that the film hinders transport of ascorbate (negatively charged interferant), without obstructing the transport of dopamine (positively charged neurotransmitter). The results are reproducible, as shown by the minimum r^2 of 0.985 for the four least squares fitted lines. The experimental reproducibility provides evidence that the deposited PPPAPA film remains adhered to gold in buffer solution.

3.3. *Chronocoulometry*

Chronocoulometry was used to determine the apparent diffusion coefficient (D_{app}) of analyte through the PPPAPA film [48]. D_{app} incorporates diffusion of analyte from bulk solution, to the solution–film interface, through the film, and to the surface of the electrode and includes diffusion, electron transfer, and ion hopping transport mechanisms. This term also includes partitioning effects, normally defined by the partition equilibrium coefficient (K_D), which relates bulk concentration to analyte concentration within the film.

Typical raw coulometric and amperometric data for a PPPAPA-coated gold electrode in 100 μM ascorbate are shown in Fig. 6. The transient charge that accumulates at the surface of the electrode, Q_t, was calculated from this raw data using the following formula: [49]

$$Q_t = Q_{raw} - \int I_{ss} dt \quad (1)$$

The steady state charge, the integral portion of the equation, was subtracted to account for double layer charging and any background oxidation. This steady state current was assumed to be constant 7 s after the potential step, indicated in Fig. 6. Conventional coulometric analysis relates the transient charge to the diffusion coefficient of the analyte by Anson's equation [50]:

$$Q_t = \frac{2nFAD_{app}^{1/2}C_b t^{1/2}}{\pi^{1/2}} \quad (2)$$

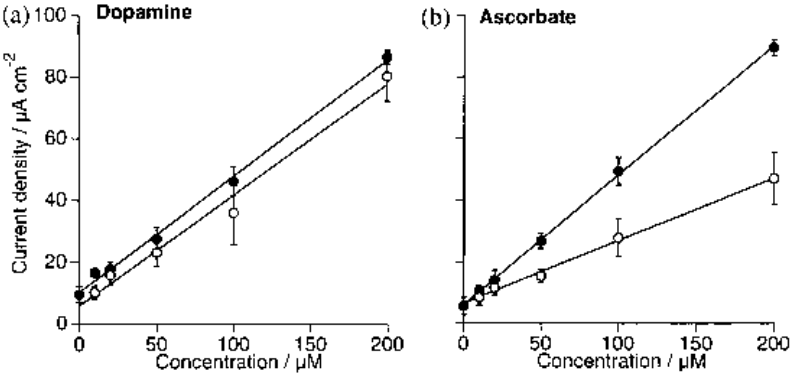

Fig. 5. Indication of PPPAPA film ionic selectivity. The diffusion-limited oxidation current density of each analyte was taken from voltammograms of the 15th scan at +350 mV vs SCE as a function of analyte concentration. The resulting slope of this plot serves as a calibration curve of the PPPAPA-coated gold electrodes to each analyte. (a) In the case of dopamine, application of the PPPAPA film reduces the response of bare gold electrodes by an average of 5%. (b) In the case of ascorbate, application of the PPPAPA film reduces the response of bare gold electrodes by an average of 50%. Key: (●) *i* (bare) and (○) *i* (film).

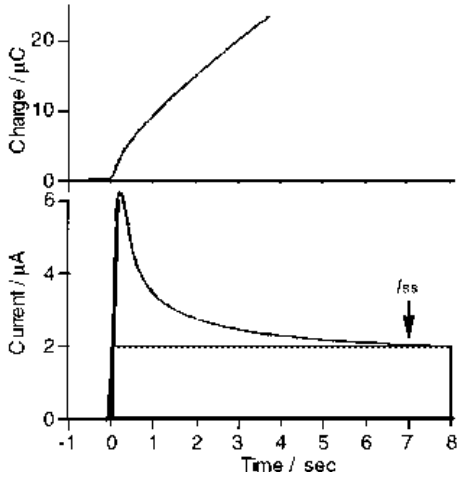

Fig. 6. Raw coulometric and amperometric data from a PPPAPA-coated gold electrode in 100 μM ascorbate. A potential step −0.05 to +0.35 V vs SCE was applied at $t = 0$. The steady state charge, calculated from integrating the steady state current, I_{ss}, is indicated in the shaded portion of the current response. The transient charge accumulated at the gold surface is calculated by subtracting the steady state charge buildup.

where n is the number of electrons transferred to the electrode, F is the Faraday constant, A is the surface area of the electrode, C_b is the analyte concentration in the film, and t is the time after the potential step.

Since this transient charge is dependent upon the concentration of bulk analyte, the transient charge is normalized to the bulk solution concentration for graphical comparison between the different analyte concentrations. A plot of the normalized charge is shown in Fig. 7 as a function of $t^{1/2}$. A small y-offset is observed, and this is attributed to capacitive charge or adsorbed electrooxidative species on the surface of the electrode [51], but should have little effect on the slope. The diffusion coefficients for ascorbate and dopamine transport through the PPPAPA film were calculated from the slope of the curves. The results, including the ratio of dopamine and ascorbate diffusion coefficients, are shown in Table 3.

Table 3. Calculated diffusion coefficient values from chronocoulometry

Concentration /μM	*Ascorbate* $10^9 D_{app}$ /cm^2 s^{-1}	*Dopamine* $10^9 D_{app}$ /cm^2 s^{-1}	$\frac{D_{app}(dopamine)}{D_{app}(ascorbate)}$
10	26 ± 6	200 ± 18*	7.6
20	26 ± 13	100 ± 26*	4.8
50	10 ± 4	18 ± 5	1.8
100	12 ± 4	29 ± 8*	2.4
200	15 ± 7	33 ± 7*	2.2

* Indicates a statistically significant difference between the dopamine and ascorbate diffusion coefficient, determined by Student's t-test p-value <0.05

4. Discussion

A few assumptions are made to calculate the apparent diffusion coefficient for the analytes through the thin PPPAPA film. Since PPPAPA is so thin, some bulk diffusion effects may be observed at the sampling rates used. However, the rate limiting step is assumed to be diffusion through the film (where $D_{app} \sim 10^{-9}$cm^{2}s^{-1}), compared with bulk solution diffusion (where $D_{app} \sim 10^{-5}$cm^{2}s^{-1}). By comparing the apparent diffusion coefficients for ascorbate and dopamine, an indication of charge selectivity can be determined.

The apparent ascorbate diffusion coefficient is significantly less than the apparent dopamine diffusion coefficient, at almost all concentrations. From the ratio of the diffusion coefficients, decreased ascorbate transport is evident. Between 50 and 200 μM, this ratio indicates that the ascorbate's diffusion coefficient is, on average, one half of dopamine's diffusion coefficient, even though both compounds have similar diffusion coefficients in water (see Table 1). This quantitatively indicates that the plasma polymerized film has improved the positively charged dopamine selectivity compared with the negatively charged ascorbate interferant.

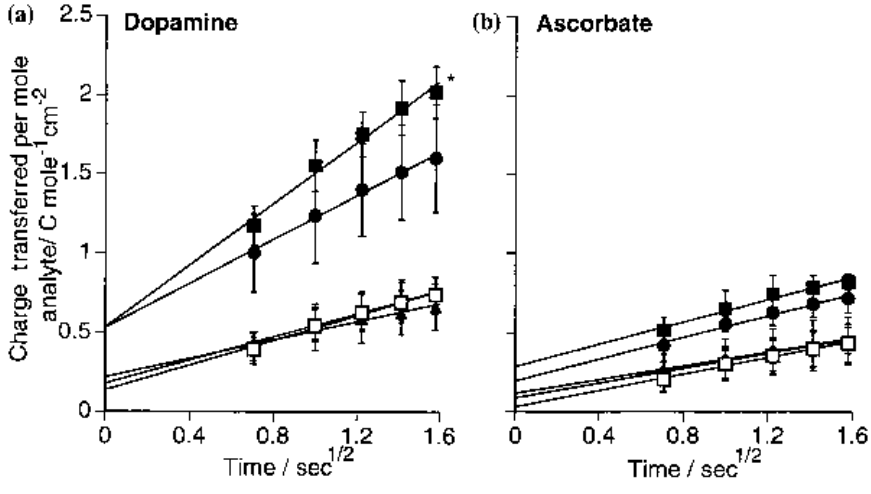

Fig. 7. Chronocoulometric response of PPPAPA-coated gold electrodes as a function of analyte concentration. A potential step –0.05 to +0.35 V vs SCE was applied at $t = 0$, and the resulting transient charge is plotted against the square root of time. The resulting slope is proportional to the diffusion coefficient of the analyte through the film. All points indicate average ± standard deviation. $n = 3$, except for* where $n = 2$. Key: (■) 10 μM, (●) 20 μM, (▲) 50 μM, (◆) 100 μM, and (□) 200 μM.

Dopamine exhibits a ten-fold higher diffusion coefficient through the PPPAPA film at 10 and 20 μM than at higher concentrations. This may be explained by modelling this system as a simple first order diffusion-limited problem. The dopamine flux, measured by chronocoulometry, is induced by the applied potential step and can be written as follows:

$$J = D_{\text{app}} \frac{(C_2 - C_1)}{d} \tag{3}$$

J is dopamine flux, C_1 and C_2 are dopamine concentrations ($C_1 < C_2$) which induce the flux, and d is the thickness of the film. The film thickness and the diffusion coefficient are assumed to be constant for all measurements, and C_1 is bound by the electrochemical reaction rate of dopamine, which is assumed to be constant for all concentrations. At high concentrations, the flux is controlled by the bulk solution concentration ($C_2 = C_{\text{bulk}}$). At lower concentrations, C_2 becomes a function of the film's ionomeric group concentration. This phenomenon, known as Donnan partitioning, causes dopamine to be electrostatically attracted to the fixed and ionized phosphonic acid moieties, thereby concentrating higher levels of dopamine in the film than in the bulk dopamine concentration [51,52]. Since all electrochemistry was performed with a strong supporting buffer (ionic strength 0.13), the concentration of dissociated ionomeric groups should be stable at all dopamine concentrations. In this case, the dissociated phosphonic acid concentration inside the film, $C_{PO_3H^-}$, should be a function of the dopamine concentration inside the film, C_2. Thus, the flux is independent of C_{bulk} and only dependent upon $C_{PO_3H^-}$. The chronocoulometry data of Fig. 7 can be used to estimate C_2, and thereby $C_{PO_3H^-}$. If the average slope for 50 to 200 μM dopamine can be used as an estimate for the actual dopamine diffusion coefficient through the film, C_2 can be calculated to be about 40 μM from the 10 and 20 μM dopamine results. Since only half of the phosphonic acid groups are ionized at pH 7.4 (pK_{a_2} of phosphonate = 7.2), only these ionized phosphonic acid groups are able to associate with dopamine. Thus the minimum effective concentration of ionomeric phosphonic acid groups is twice the measurable dopamine concentration, or approximately 80 μM. Since the actual selectivity coefficients of dopamine or other supporting electrolyte cations in the film are not known, the actual concentration of phosphate cannot be determined. However, the 80 μM provides an effective surface charge density of approximately 4 mC m^{-2}, or one charge every 40 nm^2, which is typical of other charged surfaces [53].

The calculated dopamine diffusion coefficient for the plasma polymer film is larger than reported Nafion® (shown in Table 1), while the ascorbate diffusion coefficient is larger than expected. This difference cannot be explained simply as a higher ionomeric content in Nafion®, when PPPAPA would have a smaller dopamine diffusion coefficient and a larger ascorbate diffusion coefficient than Nafion®. Examining the mechanism of ion transport in these two films provides some insight. Permselectivity of Nafion® arises from groups of ionomeric clusters separated from a hydrophobic polymer phase. In the simplest inverted-micelle model, the ionomeric spherical clusters consist of ion pairs, with polyanions forming the sphere and free cations lining the inner surface of the sphere, essentially a spherical double layer [54]. When hydrated, these clusters can increase in size and incorporate a larger number of polyanions. This double layer induces an electrostatic potential that provides the ionic selectivity. Cations require little energy to overcome this electrostatic potential to 'hop' to the next ionic cluster, while the energy barrier for the anions is prohibitive. Thus, charge selectivity improves as the electrostatic potential increases [55].

Ionomeric plasma polymerized films would not be expected to form large ionized clusters like Nafion®, due to the complex mechanism of film formation during plasma deposition. The plasma polymerized films should deposit fairly uniformly with randomly spaced ionomeric groups attached to a highly crosslinked fluorocarbon matrix. Covalent crosslinking significantly reduces conformational freedom, and ionomeric groups cannot reorganize into clusters as easily as traditionally deposited polymers like Nafion®. Individual ionized groups distributed randomly through the film are expected. Thus, PPPAPA has a more diffuse charge distribution than in Nafion® ionic clusters, resulting in an overall lower electrostatic potential. Anion selectivity is reduced by the lower potential, but the large number of ionomeric groups spread throughout the plasma film allow cations to more efficiently 'hop' from one anionic site to the next than Nafion®. Further studies are needed to explore the details of this hypothesis.

Additional experiments need to be performed in more complex media before PPPAPA films can be used as biomedical sensor coatings. Previous tests of these films in chloride solutions showed that PPPAPA films were able to reject chloride ion transport to the gold electrode surface [34]. Cycling at oxidation potentials less than gold chloride formation (~ +1.1 V vs SCE) [56] should minimize any gold chloride formation. The electrochemical response of PPPAPA in more complex systems needs to be performed, such as dopamine/ascorbate mixtures and biological media, before *in vivo* experiments can be performed. However, both the CV and chronocoulometric results provide evidence that the PPPAPA film achieves positive ion selectivity through negative ion rejection. Since plasma polymerization allows very thin films to be deposited uniformly on almost any surface, the results from this study suggest that the hydrophilic PPPAPA film possess the properties desired for an ion selective coating with little response delay. This combination of properties may have potential applications to biomedical microsensors.

5. Conclusion

A thin (~470 nm) ionomeric plasma polymerized film was successfully prepared by plasma polymerization of PAPA and was shown to have uniform coverage with good adhesion to gold surfaces. From cyclic voltammetry, the current response for gold electrodes coated with the PPPAPA film showed that the negatively charged ascorbate (interferant) response was reduced by 50% and that the positively charged dopamine (analyte of interest) response was reduced only by 5%, compared to bare gold electrodes. The diffusion coefficients of the analytes calculated by chronocoulometry showed a 50% reduction in ascorbate transport compared with dopamine, even though both compounds have similar molecular weights, sizes, and diffusion coefficients in water. These results indicate that the PPPAPA film rejects negative ions like ascorbate without significantly affecting the transport properties of positive ions like dopamine and are therefore ion-selective. This indicates PPPAPA may have promise as a biomedical sensor coating with ionic selectivity.

Acknowledgements

We would like to acknowledge financial support by NIH grant 400047 to carry out this study. We thank Drs R. Savinell, D. Gervasio and M. Danilich for their suggestions and comments.

References

[1] J. Janata, 'Principles of Chemical Sensors', Plenum Press, New York (1989).
[2] J. B. Justice, 'Voltammetry in the Neurosciences: Principles, Methods and Applications', Humana Press, Clifton, NJ (1988).
[3] R. A. Adams, *Anal. Chem*. **48** (1976) 1126.
[4] R. M. Wightman, L. J. May and A. C. Michael, *ibid*. **60** (1988) 769.
[5] M. E. Rice, A. F. Oke, C. W. Bradberry and R. N. Adams, *Brain Res.* **349** (1985) 151.
[6] I. Hu and T. Kuwana, *Anal. Chem.* **58** (1986) 3235.
[7] G. Dryhurst, K. M. Kadish, F. Scheller and R. Renneberg, 'Biological Electrochemistry', Academic Press, New York (1982).
[8] E. Palmisano and P. G. Zambonin, *Anal. Chem.* **65** (1993) 2690.
[9] R. M. Wightman, private communication, University of North Carolina at Chapel Hill (1995).
[10] P. H. Hutson and G. Curzon, *Biochem. J*. **211** (1983) 1.
[11] F. G. Gonon, C. M. Fombarlet, M. J. Buda and J. F. Pujol, *Anal. Chem*. **53** (1981) 1386.
[12] F. Malem and D. Mandler, *ibid*. **65** (1993) 37.
[13] Q. Cheng and A. Brajter-Toth, *ibid*. **67** (1995) 2767.
[14] F. Sun, D. W. Grainger, D. G. Castner and D. R. Leach-Scampavin, *Macromolecules* **27** (1994) 3053.
[15] H. -S. Yim, C. E. Kibbey, S.-C. Ma, D. M. Kliza, D. Liu, S.-B. Park, C. E. Torre and M. E. Meyerhoff, *Biosens. Bioelectron.* **8** (1993) 1.
[16] J. Janata, *Anal. Chem*. **6** (1992) 196R.
[17] R. Vaidya and E. Wilkins, *Biomed. Instrum. Technol.* **27** (1993) 486.
[18] E. W. Kristensen, W. G. Kuhr and R. M. Wightman, *Anal. Chem*. **59** (1987) 1752.
[19] J. E. Baur, E. W. Kristensen, L. J. May, D. Wiedemann and R. M. Wightman. *ibid*. **60** (1988) 1268.
[20] J. Zhou and E. Wang. *Anal. Chim. Acta* **249** (1991) 489.
[21] M. G. Gargullo and A. C. Michael, *Anal. Chem.* **66** (1994) 2621.
[22] P. S. Cahill and R. M. Wightman, *ibid*. **67** (1995) 2599.
[23] J. B. Zimmerman and R. M. Wightman, *ibid*. **63** (1991) 24.
[24] F. Moussy and D. J. Harrison, *ibid*. **66** (1994) 674.
[25] K. Pihel, Q. D. Walker and R. M. Wightman. *ibid*. **68** (1996) 2084.
[26] C. R. Martin, I. Rubinstein, and A. J. Bard. *J. Am. Chem. Soc.* **104** (1982) 4817.
[27] Z. Fan and D. J. Harrison, *Anal. Chem*. **64** (1992) 1304.
[28] D. J. Harrison, R. F. B. Turner and H. P. Baltes. *ibid*. **60** (1988) 2002.
[29] K. Yasuda, Y. Uchimoto, Z. Ogumi and Z. Takehara, *J. Electrochem. Soc.* **141** (1994) 2350.
[30] N. Inagaki, S. Tasaka, and Y. Horikawa, *J. Polym. Sci. A, Polym. Chem.* **27** (1989) 3495.
[31] M. J. Danilich, D. F. Gervasio, and R. E. Marchant, *J. Appl. Polym. Sci. Polym. Symp. (USA)* **54** (1993) 93.
[32] Z. Ogumi, Y. Uchimoto and Z. Takehara, *J. Electrochem. Soc.* **137** (1990) 3319.
[33] C. J. Brumlik, A. Parthasarathy, W. Chen and C. R. Martin, *ibid*. **141** (1994) 2273.
[34] M. J. Danilich, D. Gervasio, D. J. Burton, and R. E. Marchant, *Macromolecules* **28** (1995) 5567.
[35] M. J. Danilich, 'Functional Group Control in Radio-frequency Plasma Polymers with Biomedical Applications', Case Western Reserve University, Ph.D. thesis (1994).
[36] R. E. Marchant and I. Wang, 'Implantation Biology' (edited by R. S. Greco), CRC Press, Boca Raton (1994).
[37] W. Norde and J. Lyklema, 'The Vroman Effect' (edited by C. H. Bamford), VSP, Utrecht (1992) p. 1.
[38] J. A. Dean, 'Lange's Handbook of Chemistry', McGraw-Hill, New York (1973).
[39] S. H. Cadle and S. Bruckenstein, *Electroanal. Chem. Interfac. Electrochem.* **48** (1973) 325.
[40] R. E. Marchant, D. Yu, and C. Khoo, *J. Polym. Sci. Polym. Chem.* **27** (1989) 881.
[41] H. Yasuda, 'Plasma Polymerization', Academic Press, Orlando (1985).
[42] F. L. McCrackin, 'A FORTRAN program for analysis of ellipsometer measurements', National Bureau of Standards, Technical Note 479 (1969).
[43] S. D. Johnson, J. M. Anderson, and R. E. Marchant, *J. Biomed. Mater. Res.* **26** (1992) 915.
[44] S. D. Johnson, 'The Characterization and Biocompatibility Assessment of Plasma Polymerized Thin Films', Case Western Reserve University, MS. thesis (1993).
[45] M. E. G. Lyons, 'Electroactive Polymer Electrochemistry' (edited by M. E. G. Lyons) Plenum Press, New York (1994) p.122.
[46] L. C. Feldman and J. W. Mayer 'Fundamentals of Surface and Thin Film Analysis', New York, North-Holland (1986).
[47] M. J. Danilich, D. J. Burton and R. E. Marchant, *Vibr. Spectrosc.* **9** (1995) 229.
[48] A. R. Hillman, 'Electrochemical Science and Technology of Polymers-1' (edited by R. G. Linford), Elsevier Applied Science, London (1987).
[49] P. S. Fedkiw, S. Song, S. Sharma and J.-H. Ye, *J. Electrochem. Soc*. **142** (1995) 1909.
[50] A. J. Bard and L. R. Faulkner, 'Electrochemical Methods', John Wiley & Sons, New York (1980).
[51] Z. Gao, B. Chen and M. Zi, *J. Chem. Soc., Chem. Commun.* (1993) 675.
[52] G. Nagy, G. A. Gerhardt, A. F. Oke, M. E. Rice, R. N. Adams, R. B. Moore, M. N. Szentermag and C. R. Martin, *J. Electroanal. Chem*. **188** (1985) 85.
[53] J. Israelachvili, 'Intermolecular and Surface Forces', Academic Press Limited, San Diego (1992).
[54] T. D. Gierke and W. Y. Hsu, 'Perfluorinated Ionomer Membranes' (edited by A. Eisenberg and H. L. Yeager), ACS, Washington (1982) p. 283.
[55] V. K. Datye, P. L. Taylor and A. J. Hopfinger, *Macromolecules* **17** (1984) 1704.
[56] S. H. Cadle and S. Bruckenstein. *Electroanal. Chem. Interfac. Electrochem*. **48** (1973) 325.
[57] G. Gerhardt and R. N. Adams, *Anal. Chem.* **54** (1982) 2518.